Searching for the origins of iron technology

Ernst Pernicka, Michale Brauns, Ivan Stepanov

Curt-Engelhorn-Zentrum Archäoemtrie

The Curt-Engelhorn-Zentrum Archäometrie combines a museum institution with two universities in form of a public-private partnership.

Cooperation partners:

- **Curt-Engelhorn Foundation for the Reiss-Engelhorn-Museen**
- **University of Heidelberg**
- **University of Tübingen**
- **Klaus-Tschira Foundation**
- **Bassermann Foundation**

Early metals

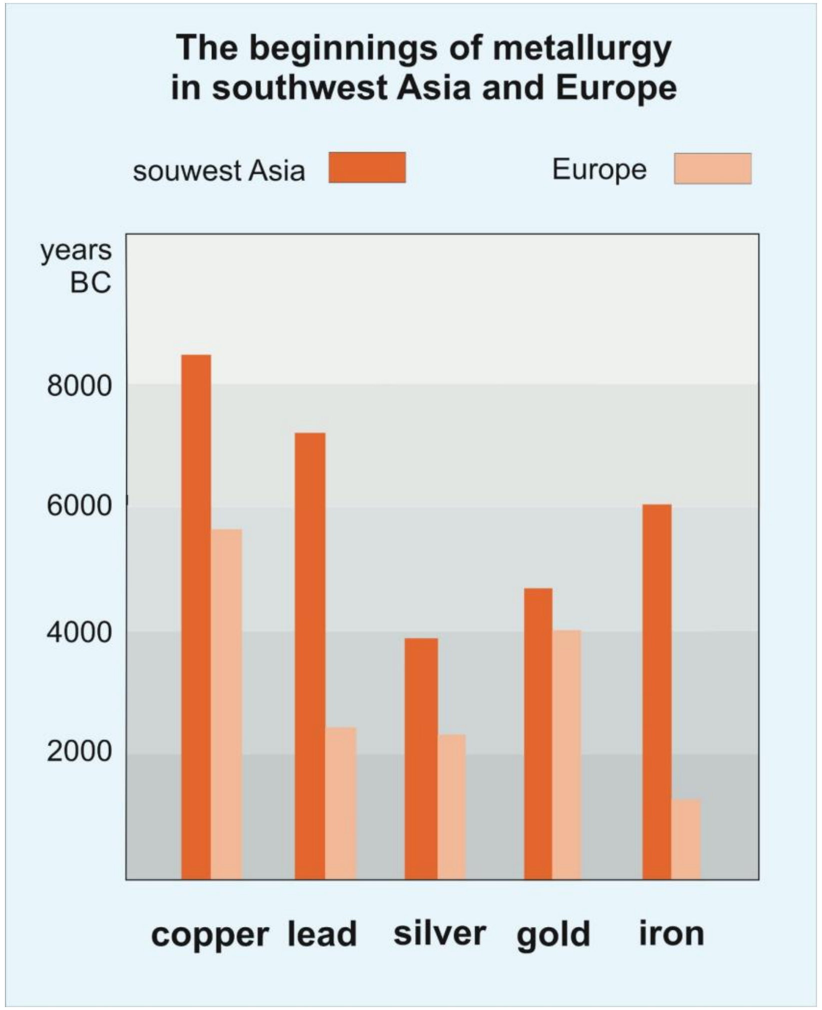

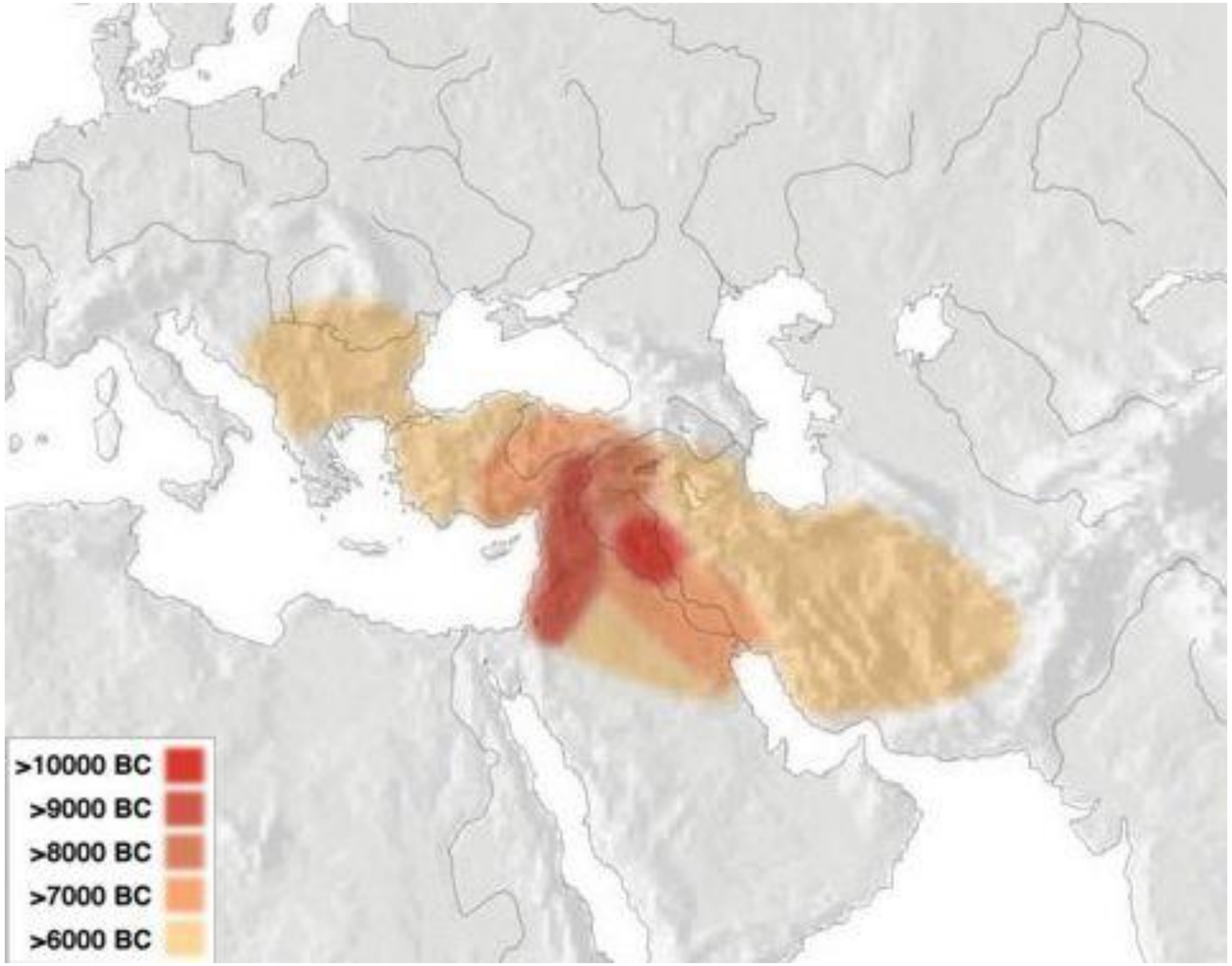

Roberts et al. Antiquity 2009

Nebra Sky Disc

The bronze was analysed for trace element concentrations and lead isotope ratios, which has become a standard approach for the determination of the provenance of base metals and their alloys.

Lead isotope ratios are less useful for gold but with SYXRF it was at least possible to determine tin concentrations in gold with high silver contents.

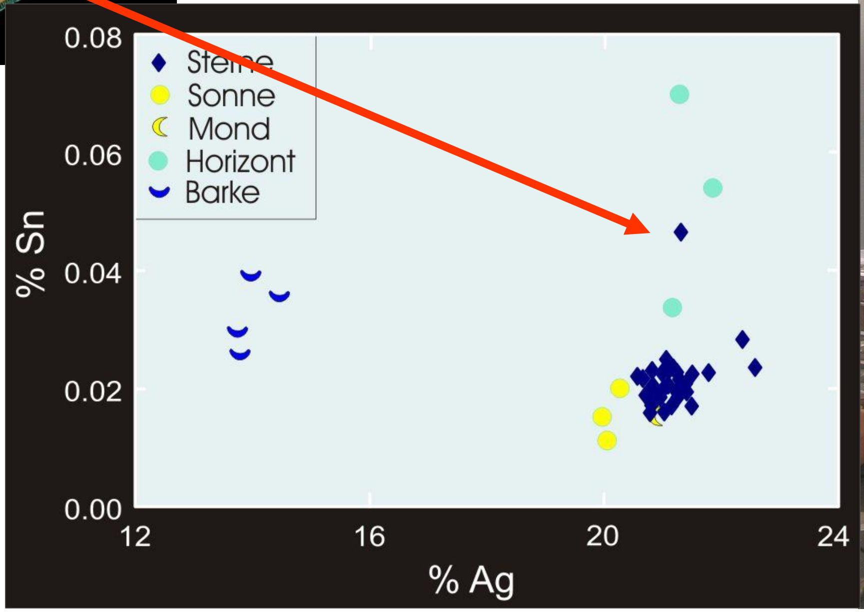

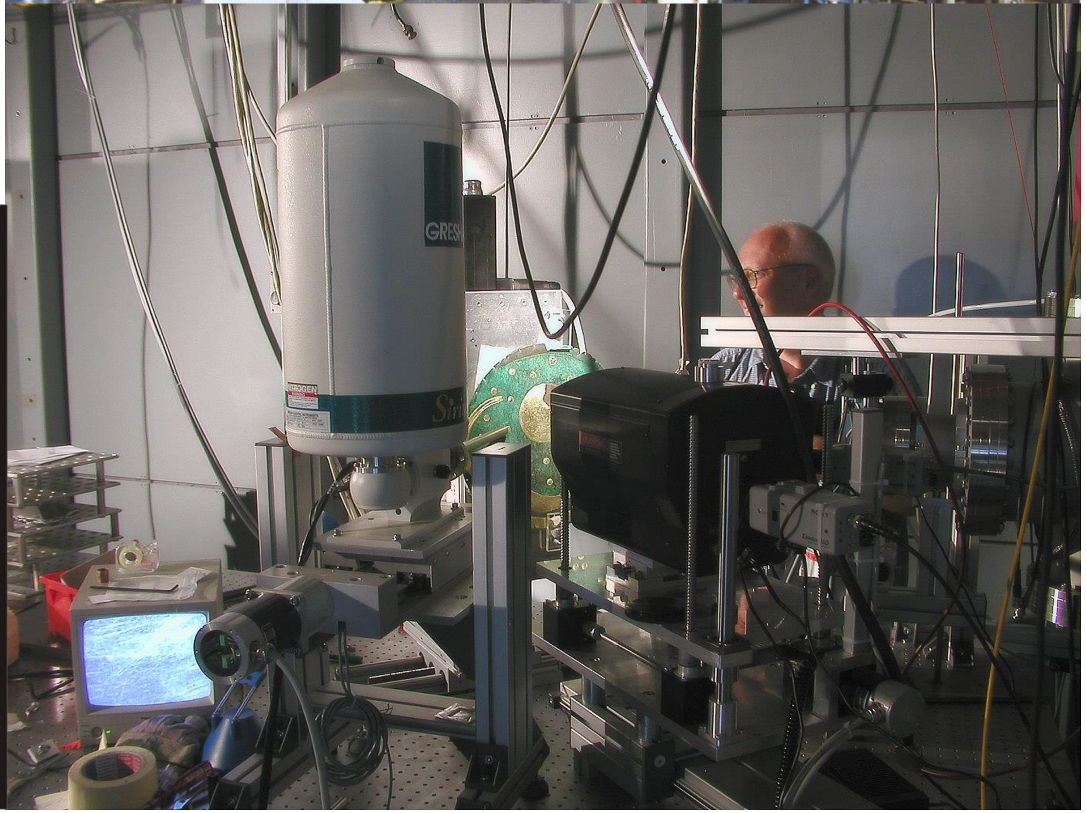

Trojan gold

For provenance analysis of prehistoric gold the sensitivity of SYXRF is not sufficient. Furthermore, the object has to be brought to the instrument. For a study on the provenance of Trojan gold a combination of mobile laser sampling with ICP-MS in the laboratory was successfully applied.

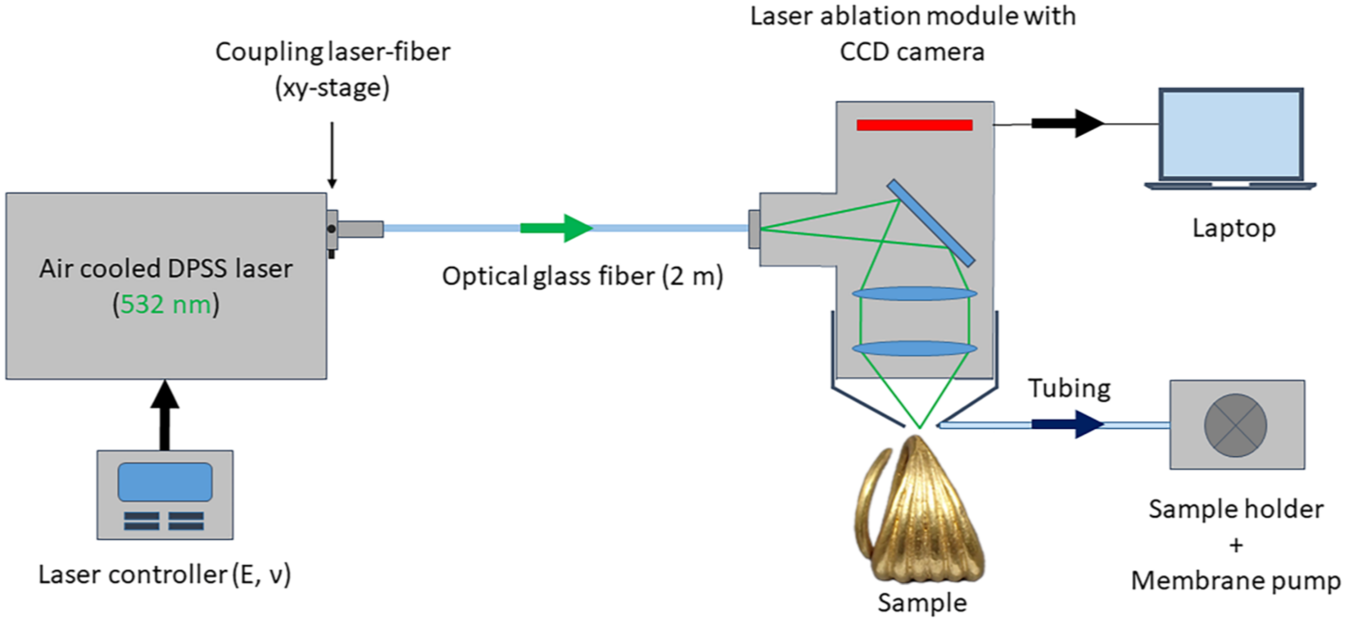

- Portable -> world-wide application
- No limits regarding the dimensions/geometry of the objects
- Quantitative analytical results on major and trace elements with low LoDs (other than XRF)
- Ablation spots non-visible with the unaided eye

Numrich et al. Journal of Archaeological Science (2023)

Trojan gold

Elements determined: Au Ag Cu Ru Rh Pd Ir Pt Mn Fe Co Ni As Cd Sn Sb Te Pb Bi Pt/Pd

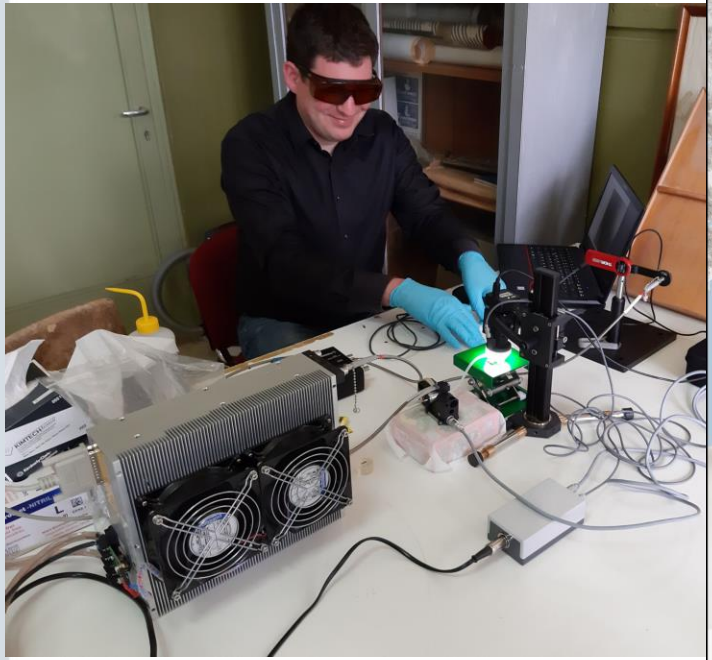

Gold objects from Troy and contemporary sites in the Aegean were compared with partly stylistically comparable gold objects from the Royal Cemetery of Ur (Jansen et al. J. Arch Science (2016), which turned out to be also compositionally similar. For the characterisation of the gold fields (yellow areas) known in antiquity, gold objects originating from these regions were used. By comparison with Trojan gold the geographically closest gold-rich regions could be excluded as possible sources. Instead, gold from the southern Caucasus has similar signature as Trojan gold, which indicates long-range transport of gold in the 3rd mill. BCE.

Early iron

Suggested spread of iron and iron production from the third to the first millennium BCE.

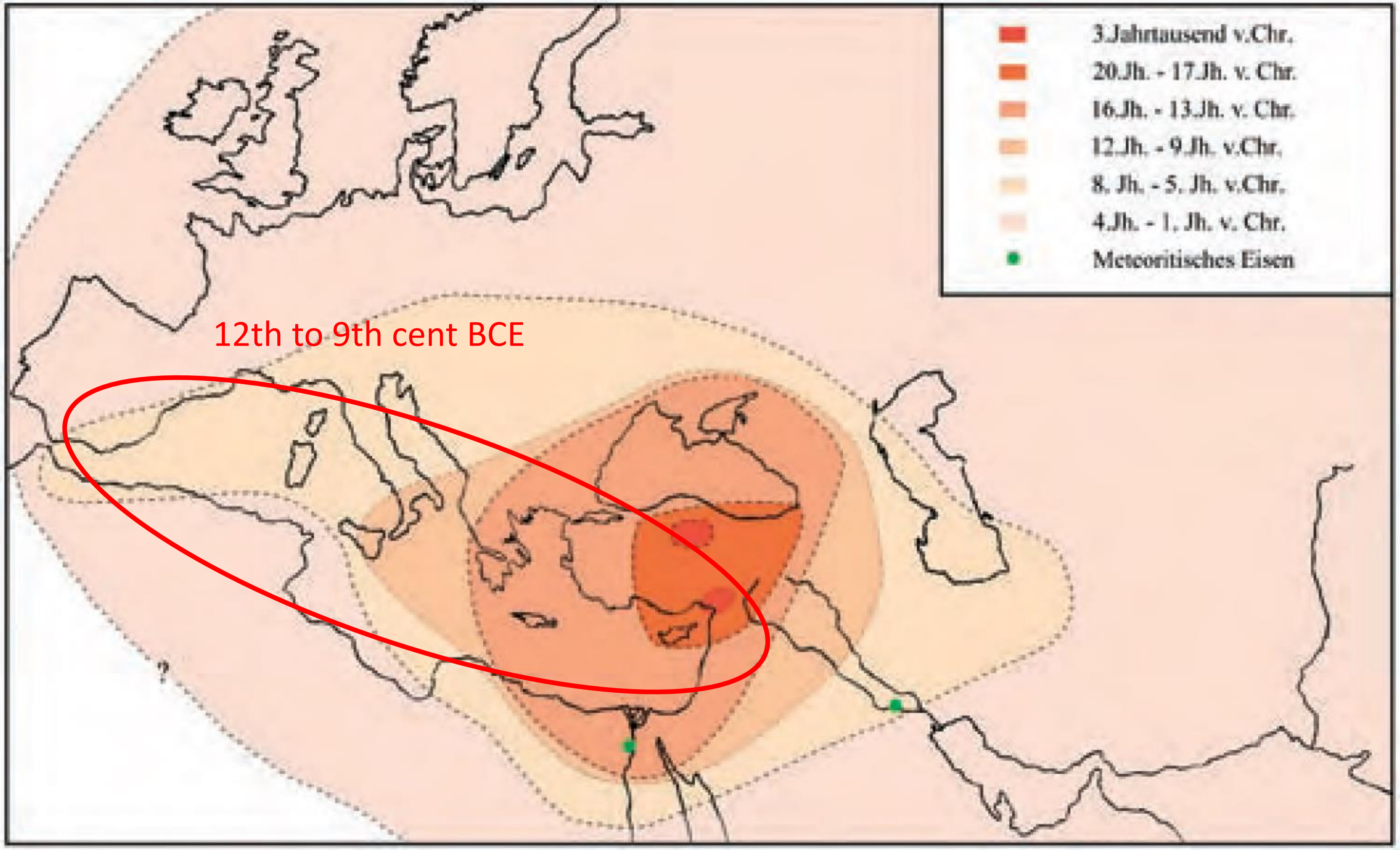

Ü. Yalcin: Zum Eisen der Hethiter (2005)

Early iron

The earliest iron objects from the sixth to the third millium BCE consist of meteoritic iron, partly confirmed by chemical analysis. For some iron objects of the third millennium BCE it remians unclear, if the consist of meteoritic or terrestrial iron, which was produced from iron ores.

The Mundrabilla iron meteorite, known mass ca. 22 tonnes

Iron dagger from Alaca Höyük (Türkiye), dated to the Early Bronze Age (2400-2300 BC) but may even date back to 2500 BC.

Early iron

The easiest identification of meteoritic iron is a high nickel concentration above ca. 8%. However, non-destructive analyses, e.g. with a portable XRF spectrometer, can lead to misleading results.

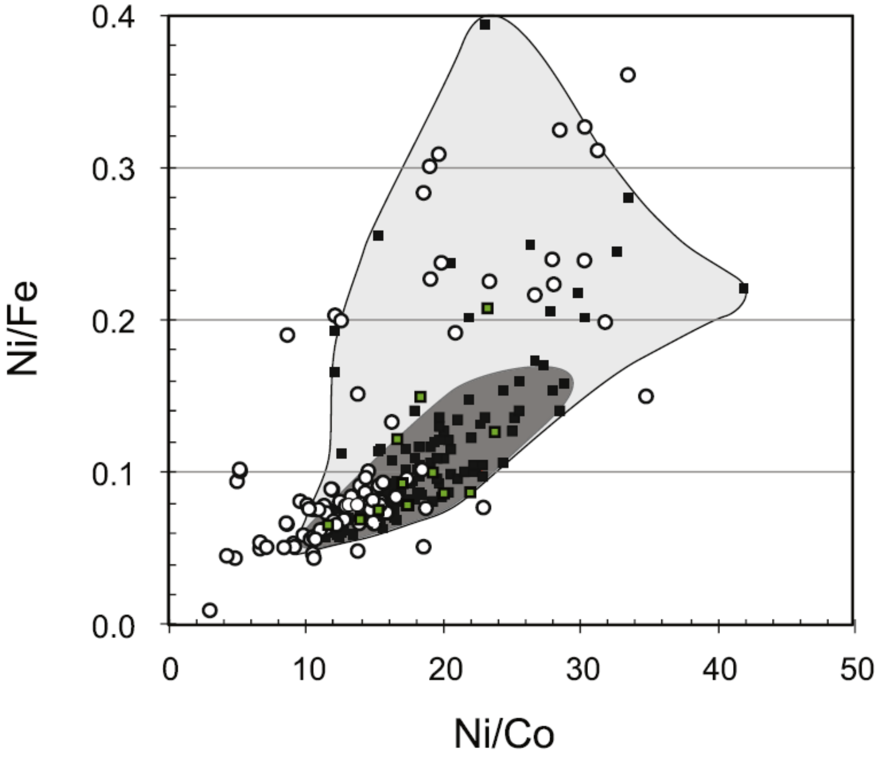

Nickel and cobalt in iron meteorites. Open symbols are pXRF analyses of fresh and oxidized surfaces (Jambon 2017)

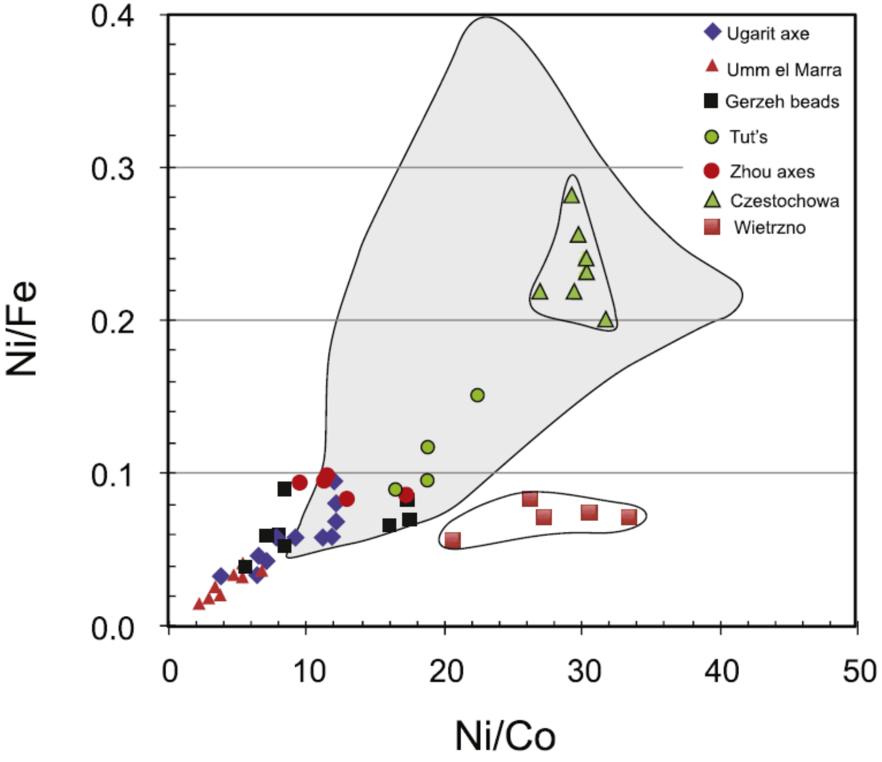

Nickel and cobalt in Bronze Age iron artefacts compared with iron meteorites (Jambon 2017)

Early iron

Early finds of iron between 1800 and 1000 BCE

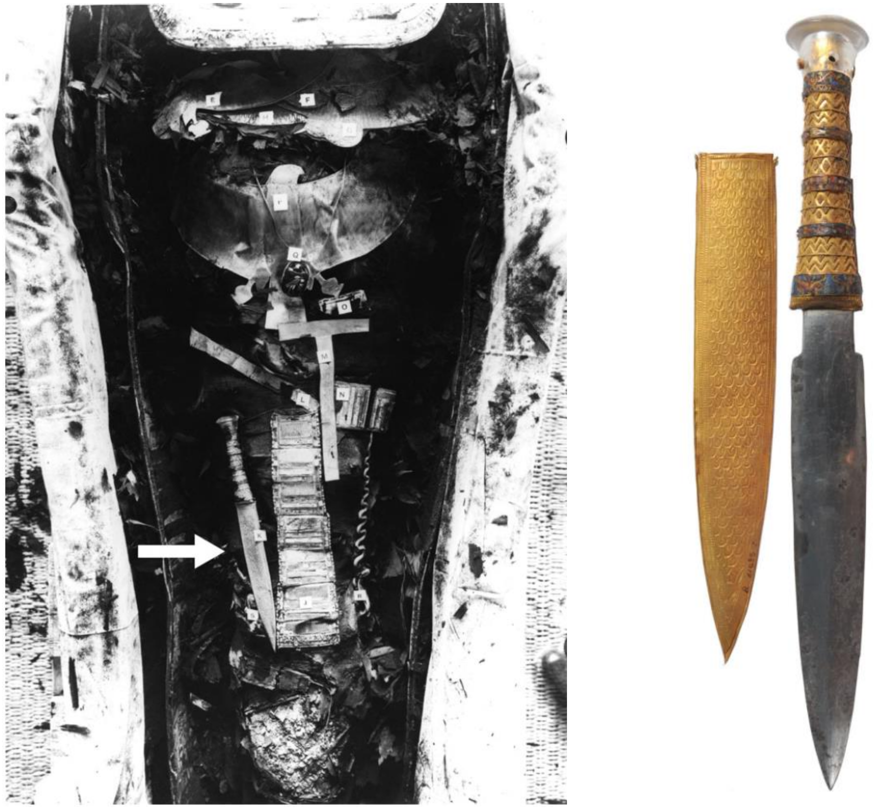

The mummy of King Tutankhamun, reigned from 1332 to 1323 BCE, iron dagger, full length 34.2 cm

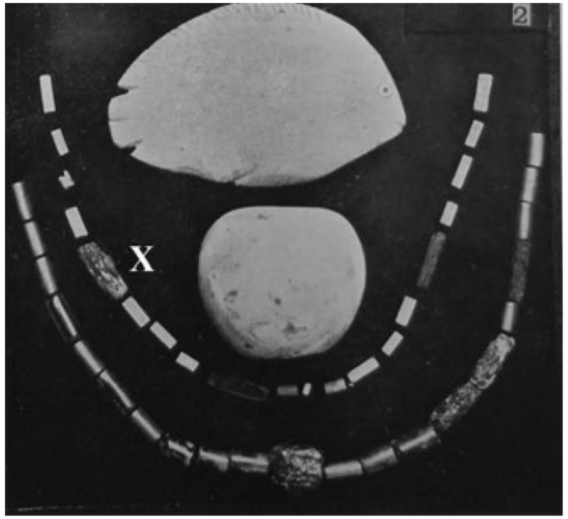

Objects from tomb 67, predynastic Gerzeh cemetery, ca. 3300 BCE

Early iron

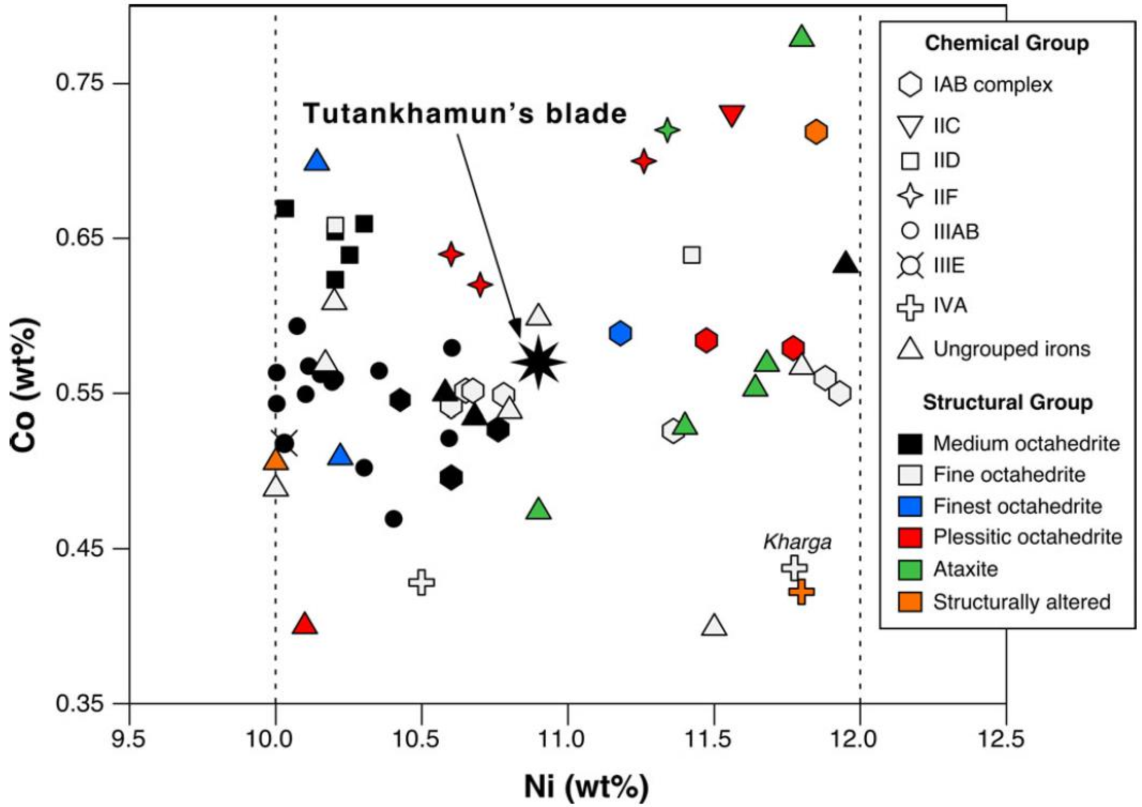

Iron meteorites with a moderately high Ni content and Tutankhamun's blade (Comelli et al. 2016)

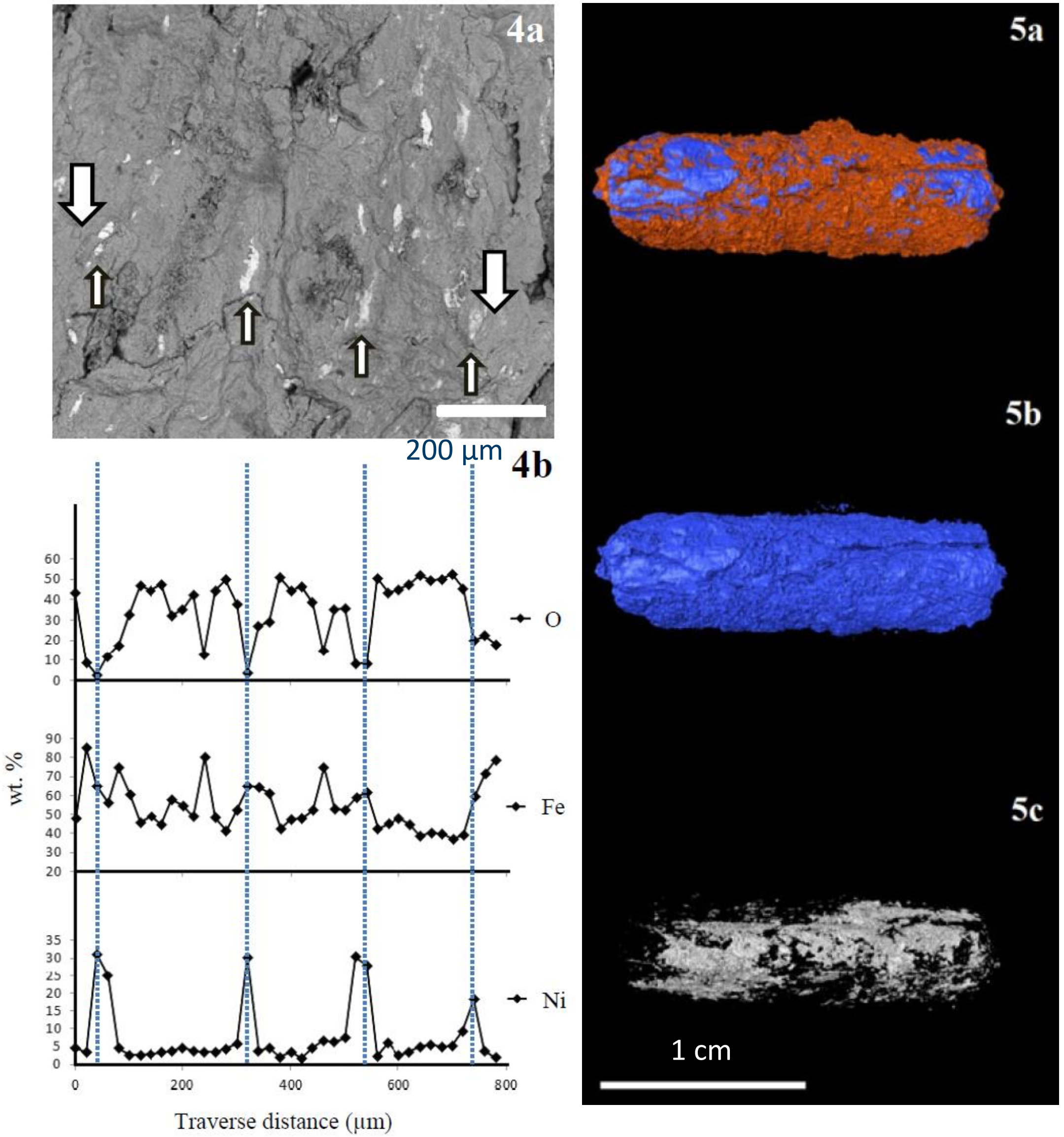

SEM-EDS analysis and CT model of the Gerzeh bead (Johnson et al. 2013)

Early iron

Spread of iron finds between 1500 and 1000 BCE

Words for iron appear in the 2nd mill BCE and especially since about 1500 BCE.

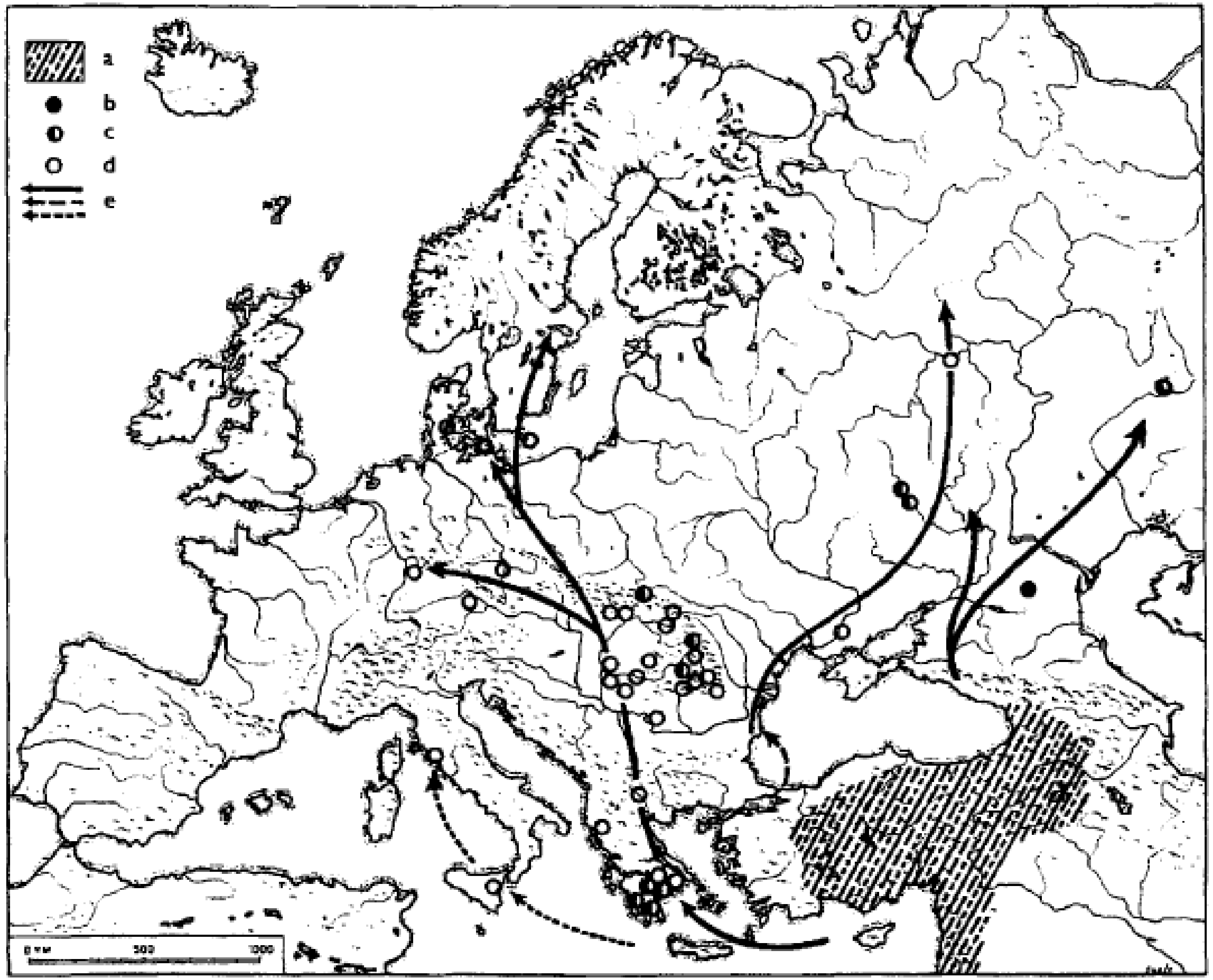

R. Pleiner: Iron in Archaeology (2000)

Early iron

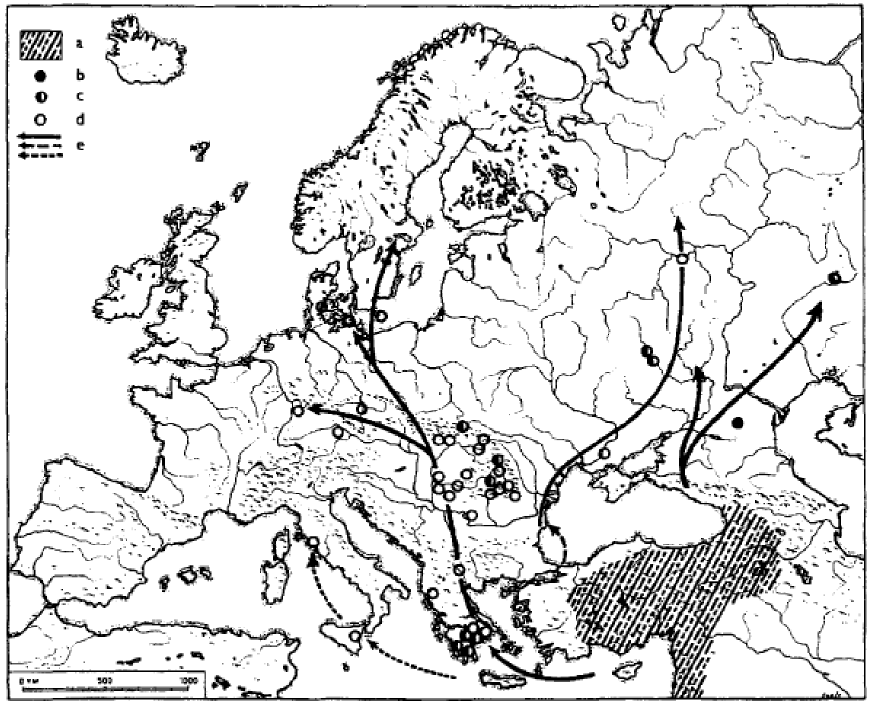

Research questions:

- Did iron production develop in the Near East or somewhere else?
- Did iron production develop in a single region or contemporaneously in different regions?
- Does the spread of iron usage indicate trade of iron or transmission of technology?

Approach:

- Chemical and isotope analysis
- Comparison of iron ores of suspected regions of origin with early iron artefacts
- Testing the compositional variability of the earliest iron objects
- Expanding the geographical and chronological range of archaeological iron objects

Early iron

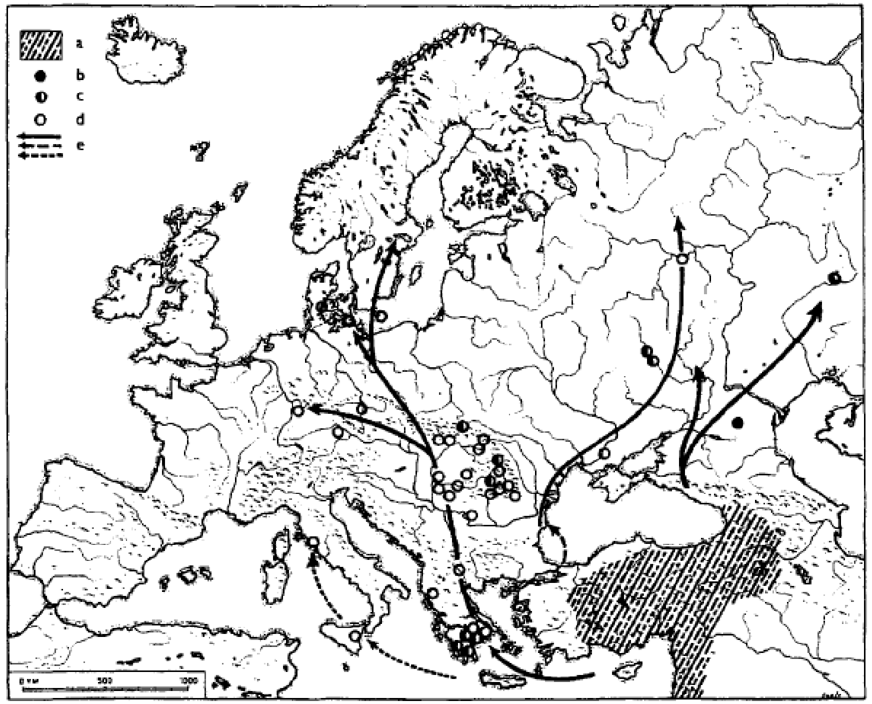

Options for the determination of the provenance of iron:

- Mn/P ratio
- Trace element concentrations in iron
- Pb isotope ratios
- Combination of Pb and Sr isotope ratios
- Cu and/or Fe isotope ratios
- Trace element concentrations in slag inclusions
- Os isotope ratios
- Os isotope ratios combined with trace element concentrations of siderophile and chalcophile elements in iron metal (Co, Ni, Cu, As, Sb, Mo, Sn)

Isotope analysis

OsO_4 (gaseous at 38°C)

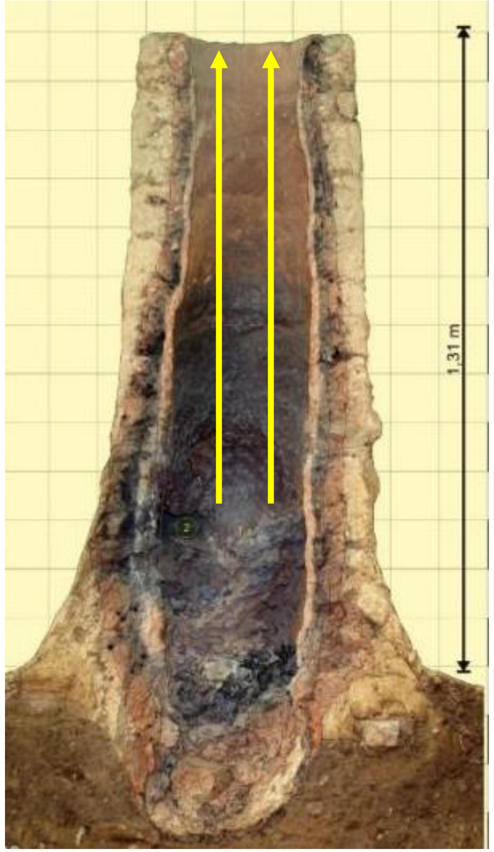

Iron ore

Fe, Sr, Os, Pb

Furnace lining
Charcoal
Fe, Sr, Pb

Os

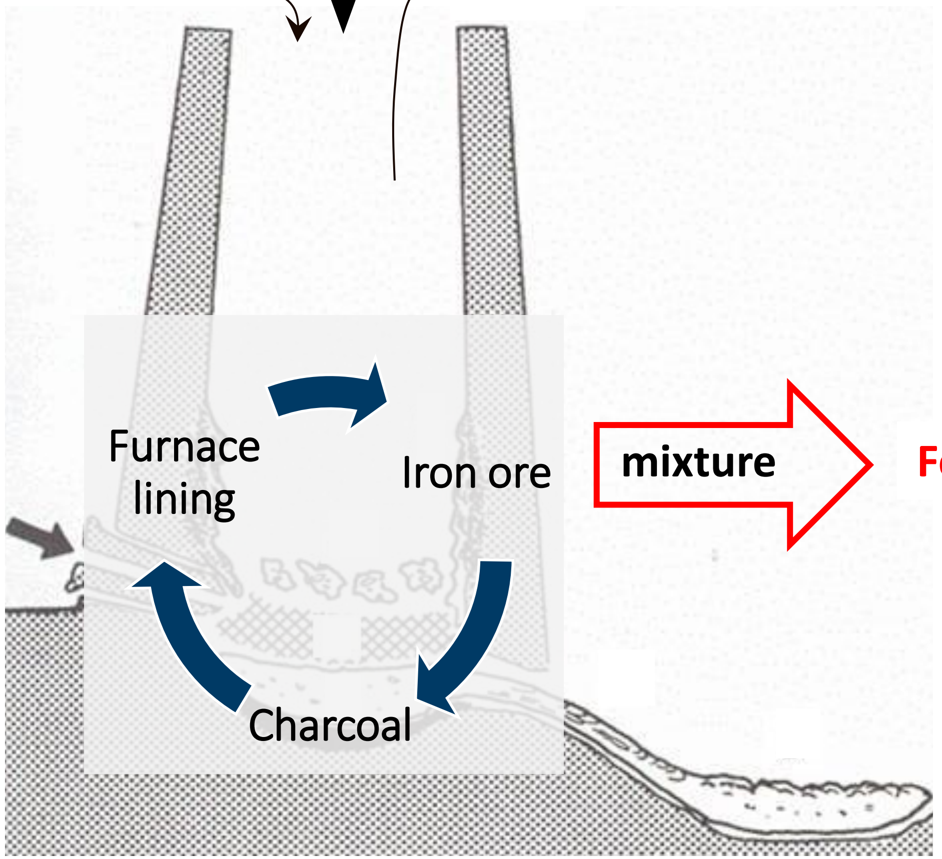

mixture

Fe, Sr, Pb

Isotope analysis

No isotope fractionation between iron ore and smelted iron

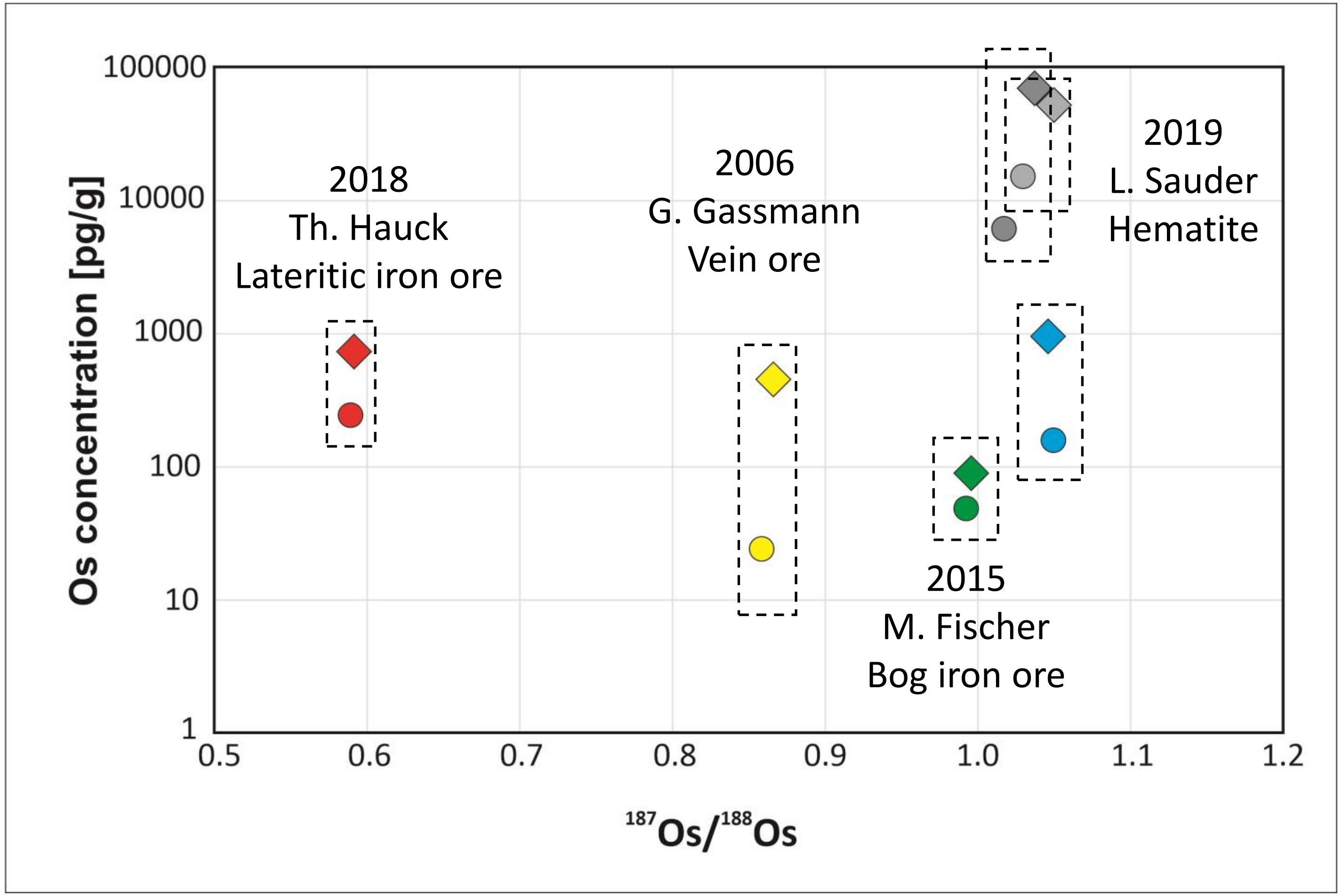

Isotope analysis

No isotope fractionation between iron metal and corrosion material, as exemplified on Iron Age iron objects from the Heuneburg (Germany)

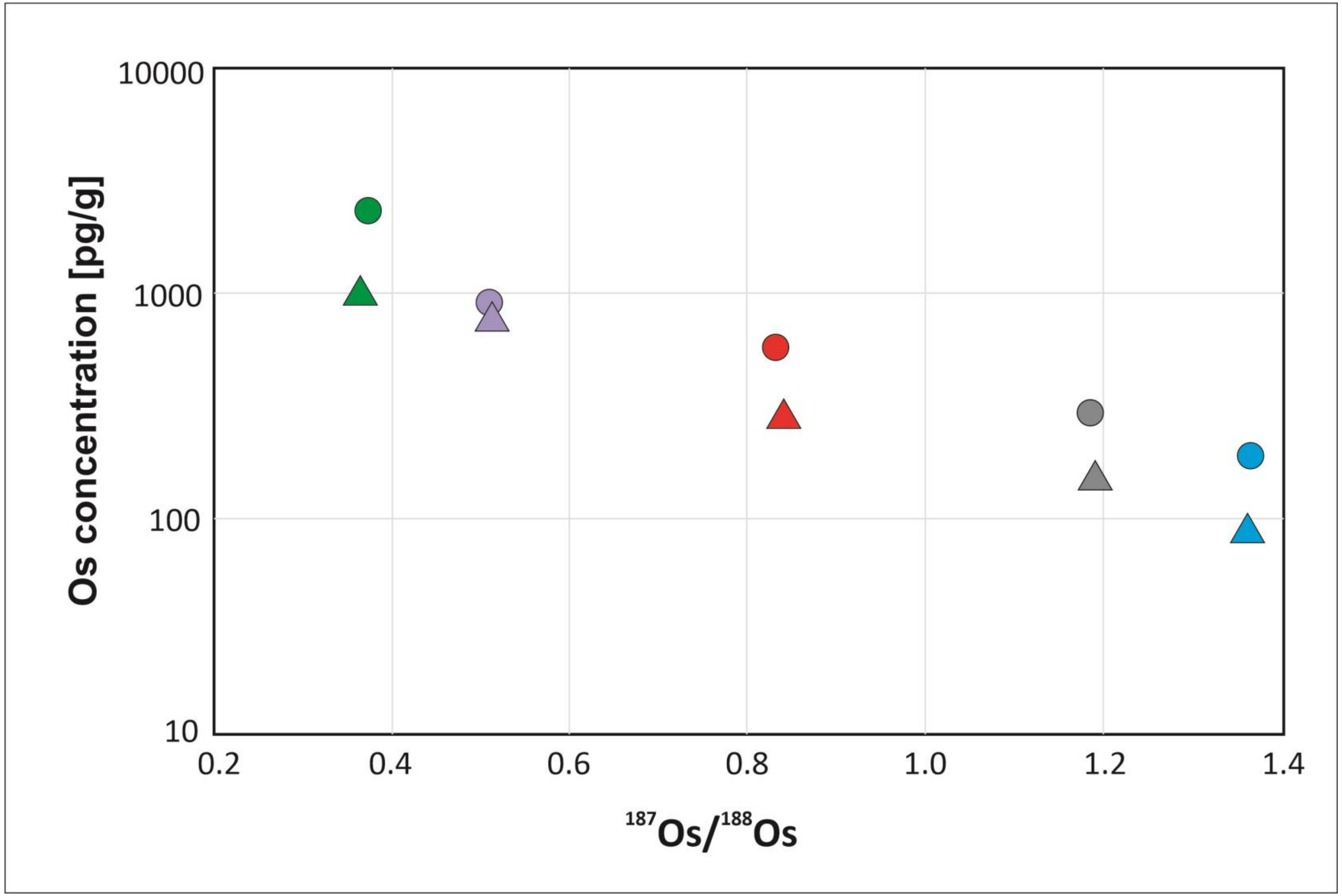

Application in Jordan

Tell Mazar cemetery, late Iron Age

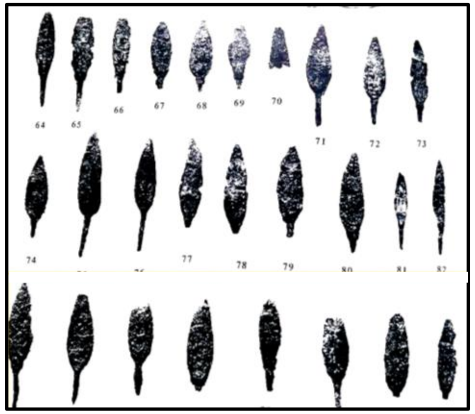

Tell Hisban settlement, Iron Age / Roman

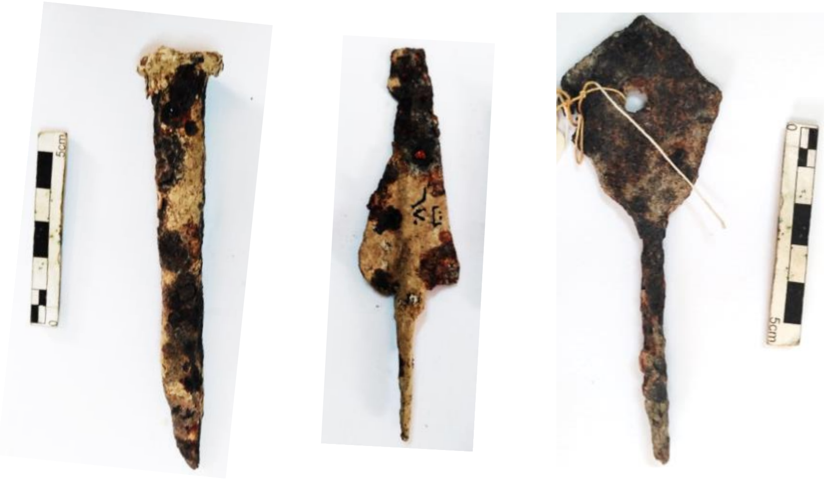

Photos (c) Courtesy Prof. Khaled Al-Bashaireh

Application in Jordan

The iron objects from Tell Mazar are not consistent with iron ores from Mugharet el-Wardeh but three objects from Tell Hisban are.

Notably, two Tell Mazar arrowheads align with copper production waste from the Faynan (Liss et al. 2020).

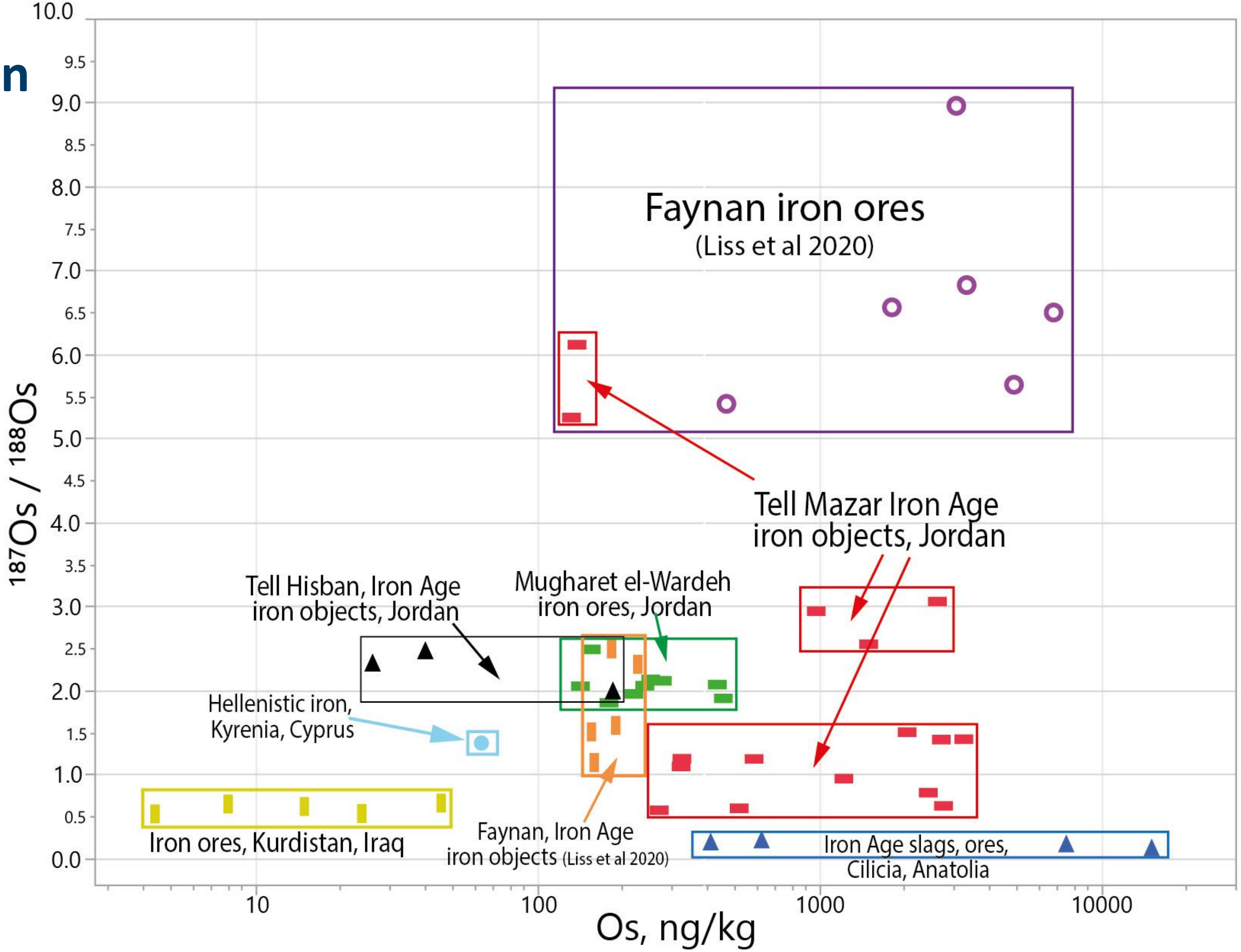

Application in Jordan

The iron objects from Tell Mazar are not consistent with iron ores from Mugharet el-Wardeh.

The relationship of two Tell Mazar arrowheads to Faynan is further supported by the trace element pattern as reported by Liss et al. (2020).

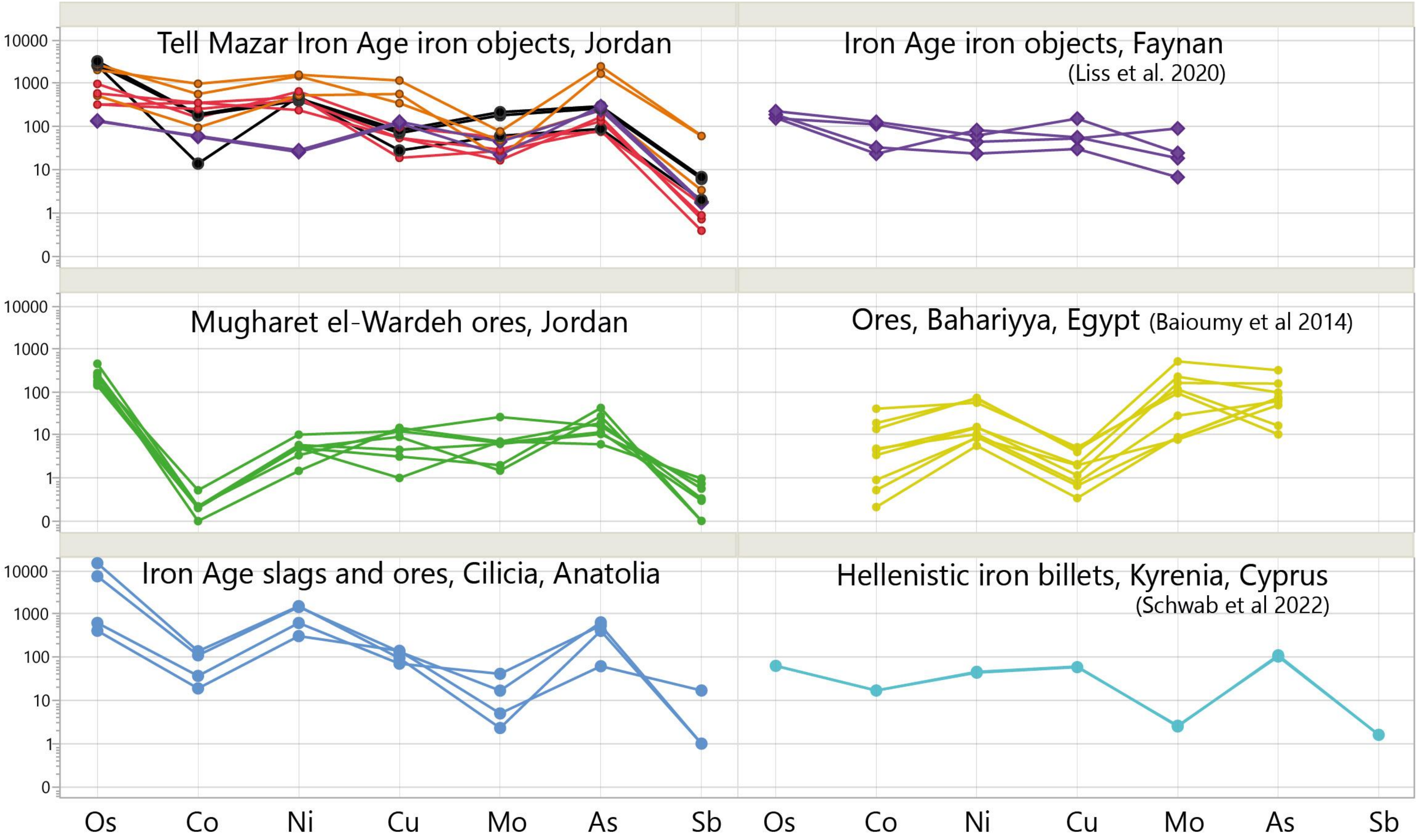

Investigation of corroded iron artefacts by X-Ray micro-computed tomography at Australian Synchrotron (ANSTO)

- Performed by Dr Anton Maksimenko (ANSTO), Dr. Filomena Salvemini (ANSTO), Ivan Stepanov (CEZA)

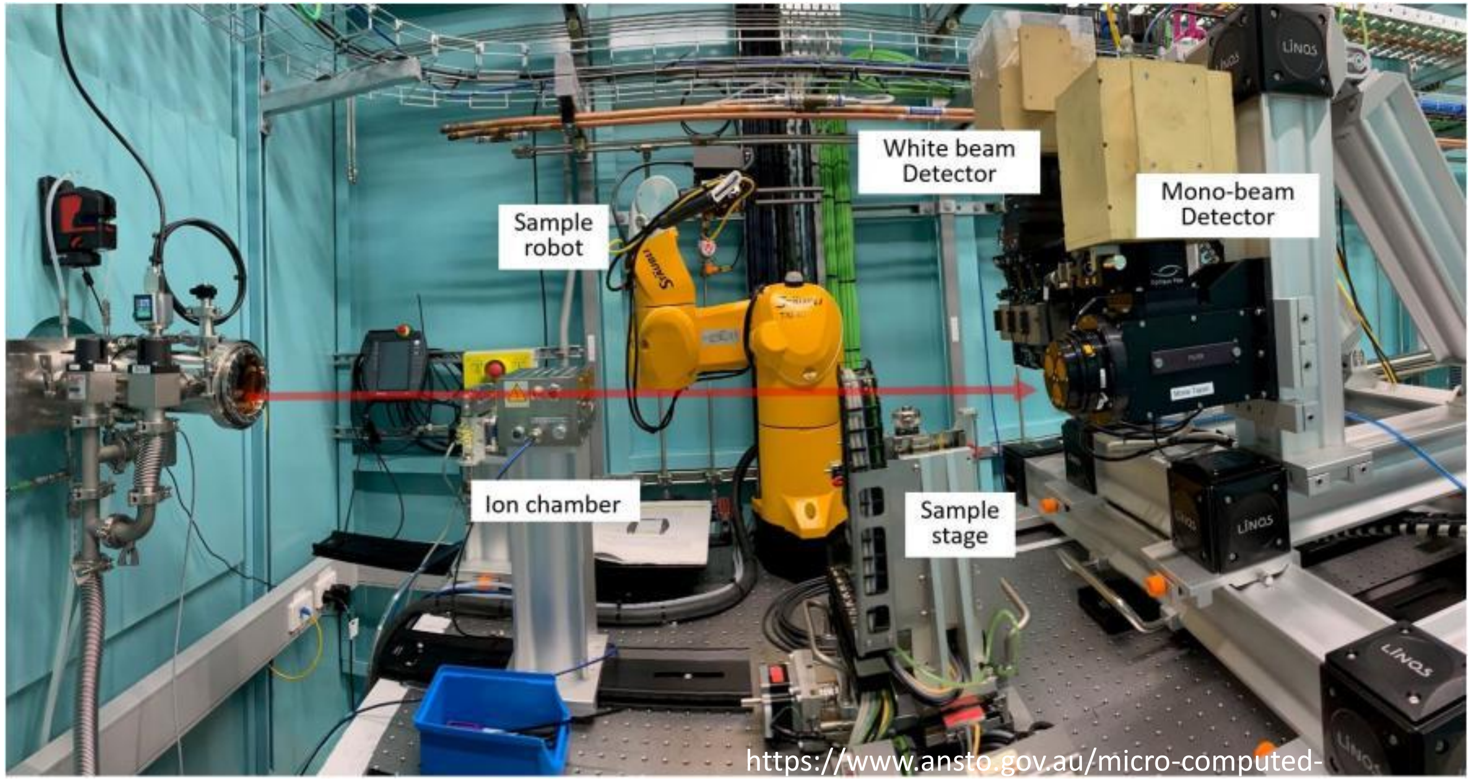

3D model

Frontal, lateral and cross-section photos of a corroded fragment of iron blade, Saruq al-Hadid, U.A.E.

X-ray Synchrotron micro-computed imaging of the Iron Age corroded iron artefact

Studied part of the object

Virtual slices in the artefact

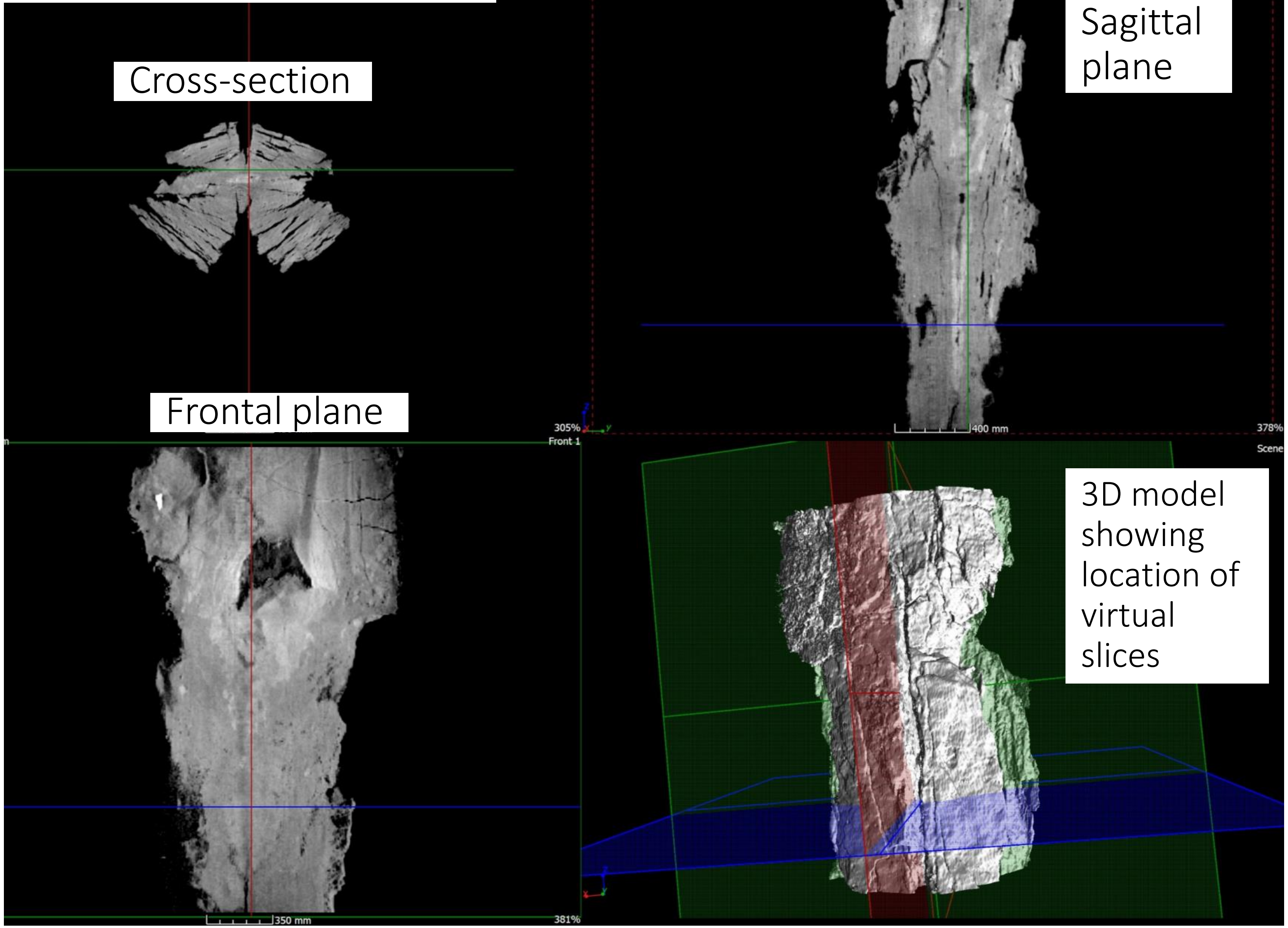

Virtual slices, past welding seams

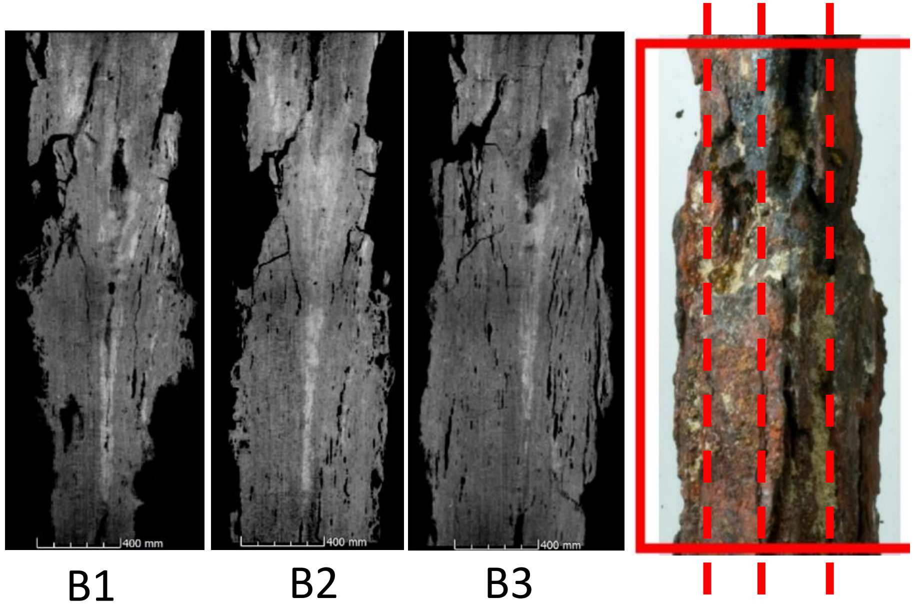

B1 B2 B3 A1 A2 A3

- Virtual slices reveal ancient welding lines allowing to understand how the object was manufactured

- The welding lines can be recognised in virtual slices due to the corrosion mechanism. The corrosion first attacked **structurally weak** parts of the artefact, resulting in development of pore networks in these areas.

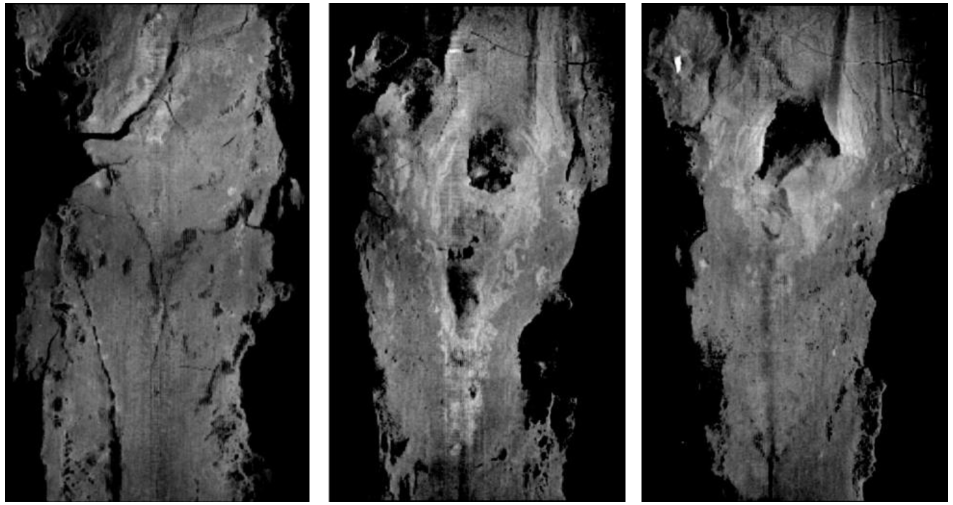

A1 A2 A3

B1 B2 B3

3d Model

Mineral phases that can be identified in X-Ray Synchrotron image

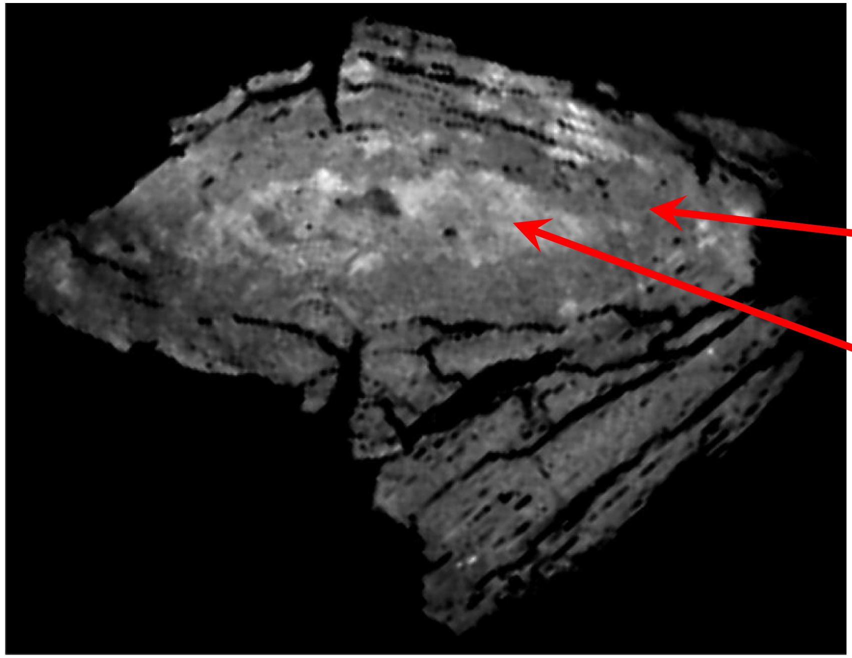

Virtual cross-section: X-Ray Synchrotron image

Metallic iron prill

Iron oxi-hydroxide: goethite (FeO*OH)

Dense corrosion product composed of Magnetite (Fe3O4 and maghemite (Fe2O4)

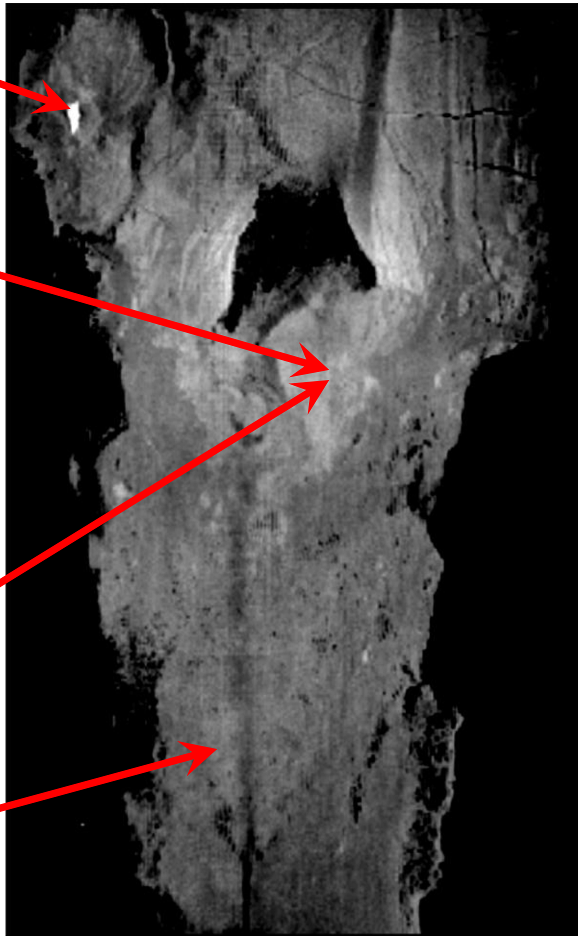

Virtual frontal-section: X-Ray Synchrotron image

Dense corrosion product composed of Magnetite (Fe3O4 and maghemite (Fe2O4)

Iron oxi-hydroxide: goethite (FeO*OH)

Metallic iron prill

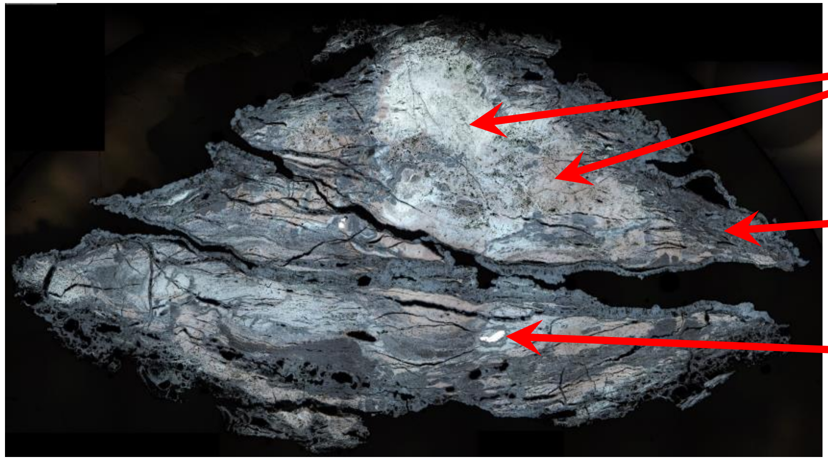

Optical microscopy image (after sectioning the object)

Results of investigation of corroded iron artefacts by X-Ray micro-computed tomography at Australian Synchrotron.

- Virtual slicing of an artefact allows to observe location of ex-welding lines in the corroded objects, helping to understand how the objects was manufactured.

- The analyses Provides sufficiently different attenuation capability to allow differentiation of metal and two principal phases of corrosion products: iron oxi-hydroxide (goethite FeO*OH) and iron oxide (magnetite Fe3O4).

- X-Rays are absorbed better by denser materials making them appear brighter on the final image. As a result, in corroded artefacts, metallic iron appears to be brighter than magnetite, while magnetite appears brighter than goethite

- Synchrotron X-Ray micro-computed tomography also bears a potential for identification of metallic prills in the matrix of corroded artefact. This information can be later used to sample the artefact in this particular area, for example for the purpose of metallographic or slag inclusion analysis.

- Compared to neutron tomography, Synchrotron X-Ray micro-computed tomography offered better resolution (c. 400 nm on Synchrotron image vs 50 µm on neutron tomographic image), and faster speed of analyses. Only several hours were required to collect all projections for a 5-cm-sized artefact at all possible angles. In contrast, c. 20 hours was needed to perform the same analytical task by neutron tomographic analyses.

CEZA